Accepted Manuscript

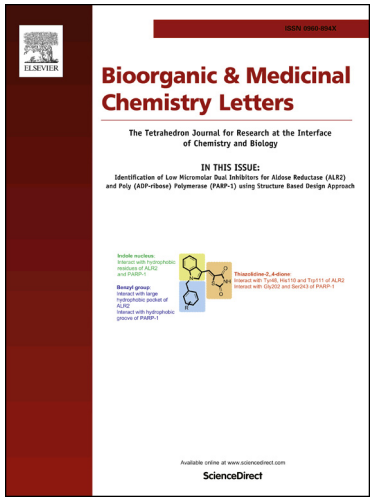

Design of potent dipeptidyl peptidase IV (DPP-4) inhibitors by employing a strategy to form a salt bridge with Lys554

Hironobu Maezaki, Michiko Tawada, Tohru Yamashita, Yoshihiro Banno, Yasufumi Miyamoto, Yoshio Yamamoto, Koji Ikedo, Takuo Kosaka, Shigetoshi Tsubotani, Akiyoshi Tani, Tomoko Asakawa, Nobuhiro Suzuki, Satoru Oi

PII: S0960-894X(17)30529-2
DOI: http://dx.doi.org/10.1016/j.bmcl.2017.05.048
Reference: BMCL 24993

To appear in: *Bioorganic & Medicinal Chemistry Letters*

Received Date: 1 February 2017
Revised Date: 9 May 2017
Accepted Date: 16 May 2017

Please cite this article as: Maezaki, H., Tawada, M., Yamashita, T., Banno, Y., Miyamoto, Y., Yamamoto, Y., Ikedo, K., Kosaka, T., Tsubotani, S., Tani, A., Asakawa, T., Suzuki, N., Oi, S., Design of potent dipeptidyl peptidase IV (DPP-4) inhibitors by employing a strategy to form a salt bridge with Lys554, *Bioorganic & Medicinal Chemistry Letters* (2017), doi: http://dx.doi.org/10.1016/j.bmcl.2017.05.048

Design of potent dipeptidyl peptidase IV (DPP-4) inhibitors by employing a strategy to form a salt bridge with Lys554

Hironobu Maezaki[a,*], Michiko Tawada[a], Tohru Yamashita[a], Yoshihiro Banno[a], Yasufumi Miyamoto[a], Yoshio Yamamoto[a], Koji Ikedo[a], Takuo Kosaka[a], Shigetoshi Tsubotani[a,b], Akiyoshi Tani[a], Tomoko Asakawa[a], Nobuhiro Suzuki[a], Satoru Oi[a,c].

[a] *Pharmaceutical Research Division, Takeda Pharmaceutical Company Limited, 26-1, Muraoka-Higashi 2-chome, Fujisawa, Kanagawa 251-8555, Japan*

[*] To whom correspondence should be addressed. e-mail: hironobu.maezaki@takeda.com

[b] *Present address: Sumika Chemical Analysis Service, Ltd. 17-85, Jusohomachi 2-chome, Yodogawa-ku, Osaka 532-8686, Japan*

[c] *Present address: Takeda Pharmaceutical Company Limited, 17-85, Jusohomachi 2-chome, Yodogawa-ku, Osaka 532-8686, Japan*

Abstract

We report a design strategy to obtain potent DPP-4 inhibitors by incorporating salt bridge formation with Lys554 in the S1' pocket. By applying the strategy to the previously identified templates, quinoline **4** and pyridines **16a**, **16b**, and **17** have been identified as subnanomolar or nanomolar inhibitors of human DPP-4. Docking studies suggested that a hydrophobic interaction with Tyr547 as well as the salt bridge interaction is important for the extremely high potency. The design strategy would be useful to explore a novel design for DPP-4 inhibitors having a distinct structure with a unique binding mode.

Keywords: dipeptidyl peptidase IV (DPP-4); S1' pocket; salt bridge formation; quinoline-based inhibitors; pyridine-based inhibitors.

Diabetes mellitus is a serious chronic disease, and an estimated 422 million adults worldwide are living with the disease as of 2014. The majority of the adults are affected by type 2 diabetes mellitus (T2DM). This used to occur mainly among adults, but now occurs in children too.[1,2] Recently, glucagon-like peptide-1 (GLP-1)-based therapy has been recognized as one of the most potential therapeutic options to treat this disorder. GLP-1 is an incretin hormone whose active form (GLP-1[7–36]amide) has multiple antidiabetic effects represented by glucose-dependent insulin secretion.[3,4] Despite the beneficial effects, active GLP-1 is rapidly inactivated by dipeptidyl peptidase IV (DPP-4, EC 3.4.14.5) known as a predominant enzyme responsible for degradation of the hormone. Therefore, inhibition of DPP-4 can prevent the degradation and maximize the antidiabetic effects.[5–7] DPP-4 is a ubiquitously distributed serine protease that cleaves dipeptides from the substrates with L-proline or L-alanine as a penultimate N-terminal residue. A number of DPP-4 inhibitors targeting the active site residues have been investigated clinically or launched as 'gliptins' so far.[8–12] Many of them were identified through peptidomimetic approaches and involve interactions with the catalytic center, i.e. Ser630. We have investigated non-peptidomimetic inhibitors having a distinct structure with a unique binding mode. Our lead generation strategy for novel DPP-4 inhibitors is as follows: novel leads would be obtained by introducing an additional interaction with S1' pocket residues into templates possessing a core heterocycle and substituents that can bind to S1 and S2 pockets adjacent to the catalytic center. In parallel, an isoquinolone derivative was selected from high-throughput screening hits as a start point that can be applied to the strategy most appropriately.[13] Scaffold hopping based on the cocrystal structure of optimized isoquinolone **1** (Protein Data Bank Code: 3OPM) led to the identification of quinoline-based and pyridine-based templates, which were proven useful for exploring novel DPP-4 inhibitors and afforded potent inhibitors forming no direct interactions toward Ser630 (e.g. **2** and **3** in Figure 1).[14–16] In the course of these studies, we envisaged that Lys554 in S1' pocket can be utilized as an unexplored target residue of DPP-4.[13,14] Although Ikuma et al. reported a docking study suggesting the interaction in 2012,[17,18] there have been no other reports that target the useful residue. Therefore, we have investigated the introduction of a salt bridge interaction with Lys554 into our templates in order to expand the applications. In this letter, we describe the designs, syntheses, and biological results of new series of DPP-4 inhibitors represented by **4**.

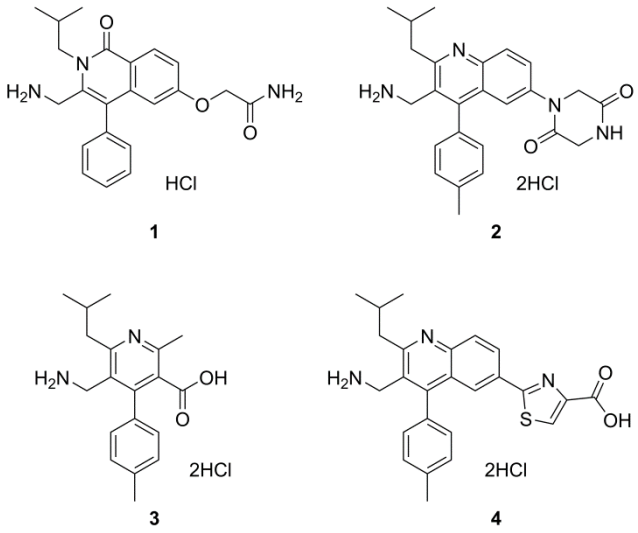

Figure 1. Representative DPP-4 inhibitors derived from scaffolds interacting with S1 and S2 pockets.

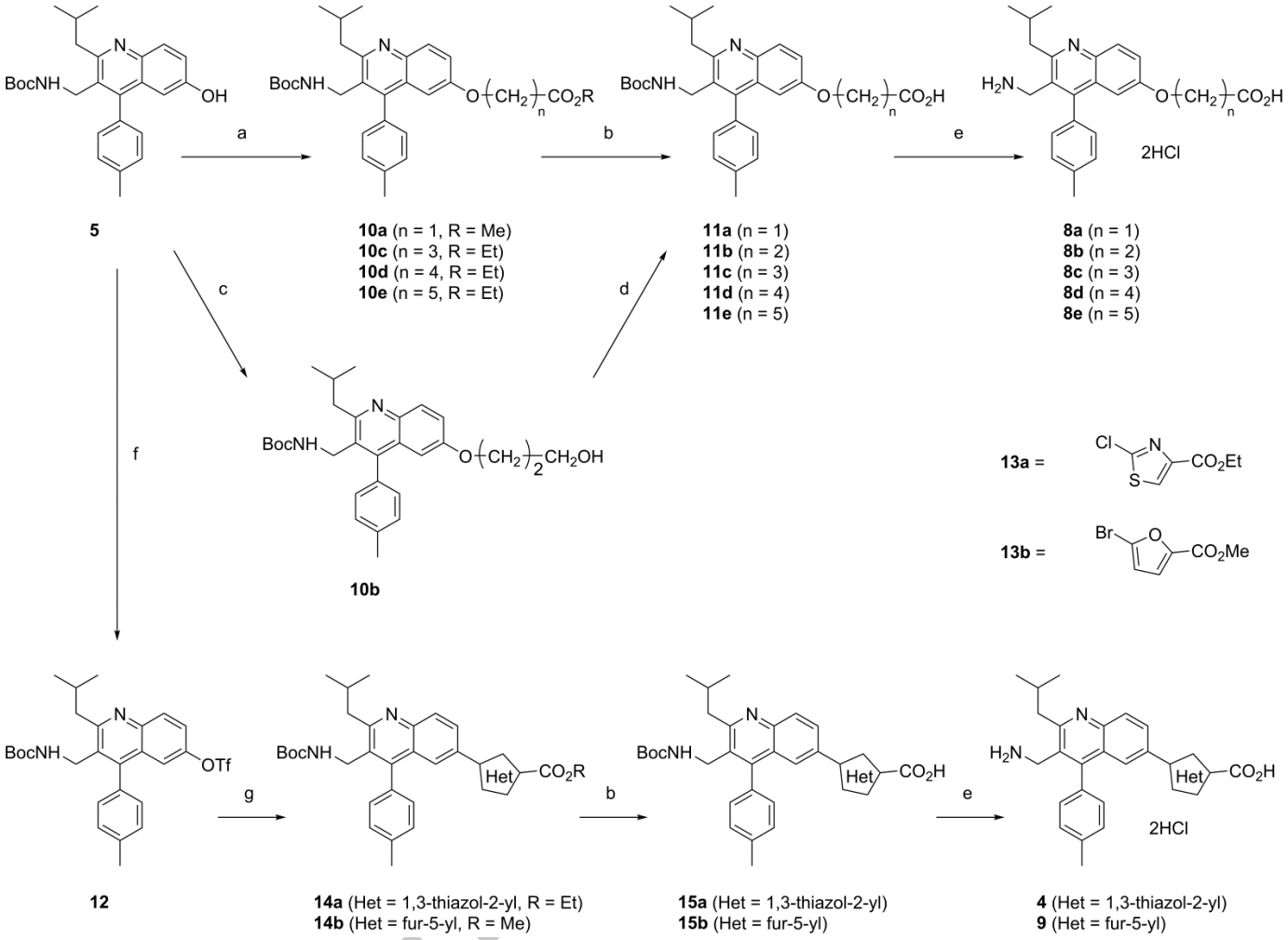

Scheme 1. Synthetic route for quinoline derivatives. Reagents and conditions: (a) halides, K_2CO_3, DMF; (b) NaOH, THF–MeOH or THF–EtOH; (c) 3-bromo-1-propanol, K_2CO_3, DMF; (d) (1) $(COCl)_2$, DMSO, CH_2Cl_2, −78 °C; (2) 2-methyl-2-butene, $NaClO_2$, NaH_2PO_4, THF–*t*-BuOH–H_2O; (e) HCl or TFA; (f) *N*-phenyl bis(trifluoromethanesulfonimide), NaH, DMF, 0 °C; (g) (1) bis(pinacolato)diboron, Pd(dppf)Cl_2·CH_2Cl_2, NaOAc, DMSO, 100 °C; (2) **13a** or **13b**, $Pd(PPh_3)_4$, K_2CO_3, toluene–MeOH–H_2O, reflux.

The starting materials **5** and **6** and the intermediate **7** shown in Schemes 1 and 2 were prepared using the previously reported procedures.[14,15,19] As shown in Scheme 1, quinoline-based carboxylic acids **8a–e** were obtained by alkylation of **5** followed by alkaline hydrolysis of esters of **10a** and **10c–e** or oxidation of **10b** and subsequent *N*-Boc deprotection of **11a–e**. Suzuki coupling of triflate **12** prepared from **5** with commercially available halides **13a** and **13b** provided esters **14a** and **14b**, respectively. Saponification of **14a** and **14b** followed by *N*-Boc deprotection gave the desired **4** and **9**, respectively. Synthesis of pyridine derivatives is outlined in Scheme 2. Oxidation of pyridin-3-ylmethanol **7** and subsequent Wittig reaction with a phosphonium salt prepared from ethyl 2-chloro-1,3-thiazole-4-carboxylate (**19**) afforded ester **20a**, which was

hydrogenated over palladium on carbon to yield ester **20b**. Ether **22** was obtained by mesylation of **7**,

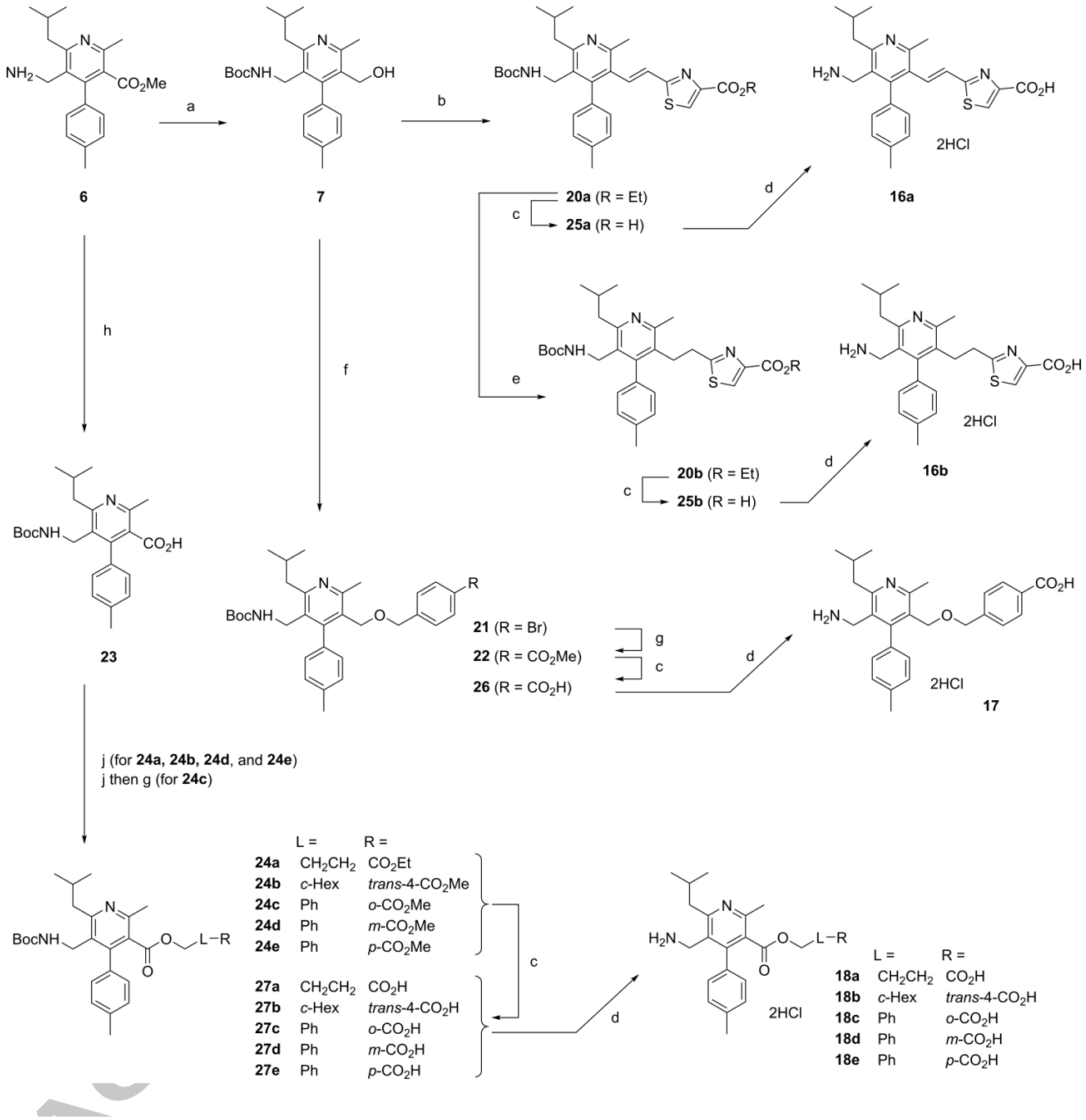

Scheme 2. Synthetic route for pyridine derivatives. Reagent and conditions: (a) (1) DIBALH, toluene, −78 to 0 °C; (2) Boc_2O, NaOH; (b) (1) Dess–Martin reagent, CH_2Cl_2, (2) ((4-(ethoxycarbonyl)-1,3-thiazol-2-yl)methyl)(triphenyl)phosphonium bromide, NaH, DMF; (c) NaOH, THF–EtOH or THF–MeOH; (d) HCl or TFA then HCl; (e) 10% Pd on charcoal, H_2, EtOH; (f) (1) MsCl, NEt_3, THF; (2) (4-bromophenyl)methanol, NaH, THF: (g) CO_2, $Pd(dppf)Cl_2{\cdot}CH_2Cl_2$, NEt_3, MeOH–DMF, 80 °C; (h) (1) Boc_2O, THF; (2) NaOH, MeOH, reflux; (j) halides or mesylate, K_2CO_3, DMF.

alkylation with 4-bromobenzyl alcohol, and palladium-catalyzed carbonylation using CO_2. For the synthesis of a series of nicotinates **18a–e**, the starting nicotinate **6** was hydrolyzed and protected by a Boc group to yield

23, which was re-esterified to afford **24a**, **24b**, **24d**, and **24e**. For **24c**, further esterification of the obtained 4-bromobenzyl ester was performed by palladium-catalyzed carbonylation using CO_2. The esters **20a**, **20b**, **22**, and **24a–e** were converted to the desired acids **18a–e** by alkaline hydrolysis and subsequent *N*-Boc deprotection. Carboxamides **28a–c** corresponding to carboxylic acids **11d**, **15a**, and **25b**, respectively, were prepared using a general coupling procedure followed by acidic *N*-Boc deprotection.

The synthesized compounds were evaluated for their in vitro inhibition against human DPP-4 using Gly-Pro-*p*-NA as a substrate. IC_{50} results analyzed with sigmoidal dose response curves are outlined in Tables 1 and 2. To seek DPP-4 inhibitors that can form a salt bridge with Lys554, quinolines with a terminal carboxy group in the 6-substituent were evaluated (**8a–e** in Table 1). The results indicated that the activity increased as linker length elongated. The optimal **8d** (n = 4) exhibited 30-fold more potent inhibition than **8a** (n = 1). Based on the reported X-ray cocrystal structure of isoquinolone-based inhibitor **1** bound to DPP-4,[13] the distance from the oxygen atom at the 6-position of isoquinolone **1** to the terminal amino group of Lys554 is around 6.6 Å. Assuming that quinolines **8** take the similar binding mode to that of isoquinolone **1**, the optimal chain length in quinolines **8** would be that of **8a** (n = 1) in an extended form. Therefore, the linker length of the most potent analogue **8d** (n = 4) seemed too long to allow the carboxy group to interact with Lys554. To understand the potent DPP-4 inhibition of **8d**, docking study was performed based on the cocrystal structure of **1**. The study provided multiple conformations and the most appropriate binding mode is displayed in Figure 2. In the model, **8d** could adopt an essentially similar binding mode to the previously reported for other quinoline derivatives.[14] The result suggested that the relatively long linker

Table 1. SAR Summary of Linkers (L) in Quinoline-based Carboxylic Acids

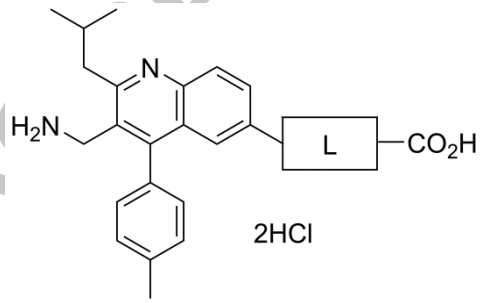

Compound	L		DPP-4 IC_{50} (nM)[a]
8a	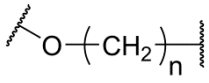	n = 1	140
8b		2	29
8c		3	17

8d		4	4.6
8e		5	6.8
9	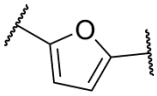		28
4	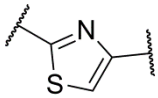		0.38
1[b]			220
3[b]			22

[a] Inhibitory activity against human DPP-4 was measured using Gly-Pro-pNA as a substrate. [b] Free bases of **1** and **3** were used as positive controls.

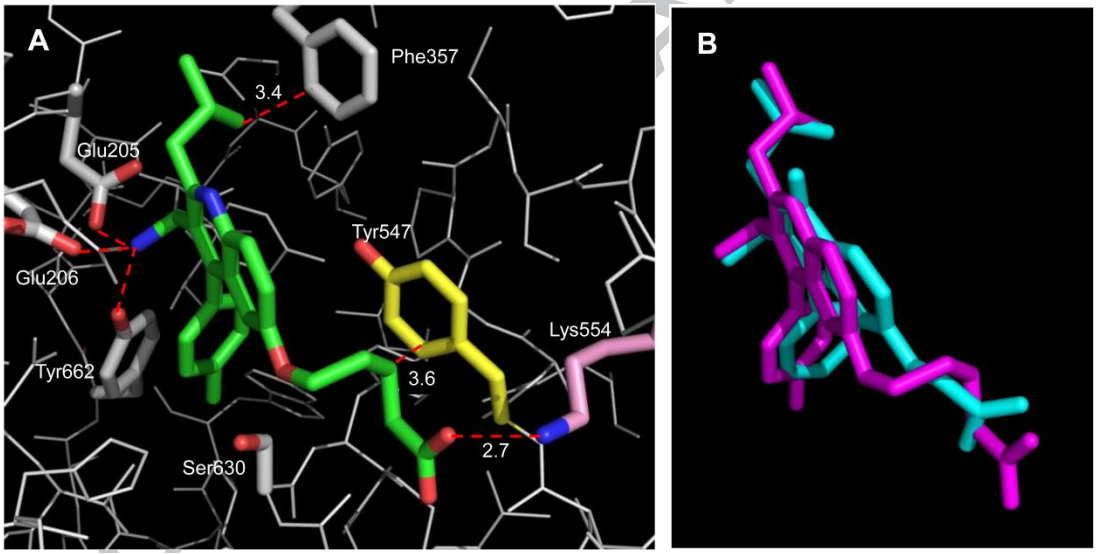

Figure 2. Docking study between compound **8d** and DPP-4 protein. (A) Lys554 (pink), Tyr547 (yellow), and other amino acids (gray) in the binding site of **8d** (green carbons). Major interactions are depicted as red dotted lines. Distances in angstroms. (B) Superimposition of **8d** (magenta) onto X-ray cocrystal structure of **1** (cyan).

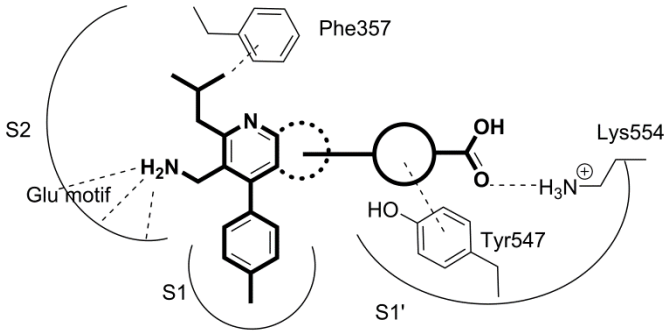

Figure 3. Proposed pharmacophore using quinoline-based or pyridine-based scaffold involves a hydrophobic interaction with Tyr547 to efficiently form a salt bridge with Lys554.

was packed within the space of S1' pocket by curving the chain. It was anticipated that flat aromatic ring linkers instead of the long linear linkers would enable the carboxy group to locate at the suitable position for Lys554 by the support of the interaction with Tyr547. Therefore, compounds incorporating the aromatic ring linker moiety were hypothesized to achieve highly efficient binding to the enzyme. Based on the hypothesis, we constructed a new pharmacophore using the quinoline and pyridine cores substituted with 3-aminomethyl, 2-isobutyl, and 4-*p*-tolyl groups as templates (Figure 3).

First, the ring linker was introduced to the 6-position of the quinoline template. On the basis of the above-mentioned results of docking studies, five-membered heteroaromatic rings were selected as a linker at the 6-position to orient the carboxy group toward the amino side chain of Lys554. 2-Furoic acid **9** and thiazole-4-carboxylic acid **4** were evaluated for the DPP-4 inhibitory activity. As shown in Table 1, compounds **9** and **4** were found to be potent inhibitors. Remarkably, **4** exhibited highly potent subnanomolar inhibitory activity (IC_{50} = 0.38 nM), which is the highest potency of this series.

For further simplification, we applied the pharmacophore model to the pyridine-based template. The high inhibitory activity of quinoline **4** was retained by ring-opened analogues **16a** and **16b**, which were identified to be nanomolar inhibitors (Table 2). In contrast, a lack of the heteroaryl linker resulted in a dramatic decrease in potency (**18a**). By replacing the alkyl linker of **18a** with a benzene ring, benzyl esters **18c**, **18d**, and **18e** showed 5- to 30-fold more potent inhibitory activity. Replacement of the linker with a cyclohexane ring also resulted in ca. 6-fold potency increase (**18b**) when compared with **18a**. The activity was slightly emphasized by increasing flexibility of the linker in **18e**, and ether **17** demonstrated a nanomolar inhibition. These results indicate that general hydrophobic rings, such as an aryl and cycloalkyl, could be incorporated as a linker to enhance the inhibitory activity of carboxylic acid derivatives as well as a thiazolyl linker.

Table 2. SAR Summary of Linkers (L^1 and L^2) in Pyridine-based Carboxylic Acids

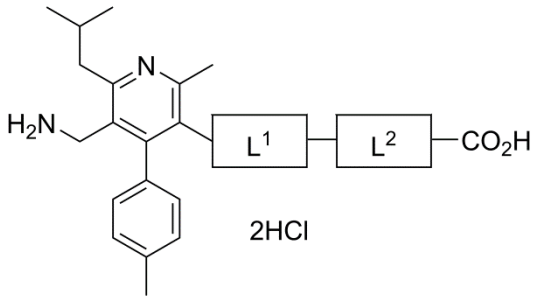

Compound	L^1	L^2		DPP-4 IC_{50} (nM)[a]
16a	(*E*)-CHCH	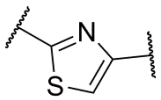		5.5
16b	CH_2CH_2	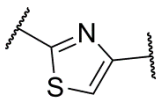		2.6
18a	CO_2CH_2	CH_2CH_2		470
18b	CO_2CH_2	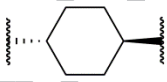		80
18c	CO_2CH_2	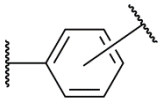	*ortho*	29
18d	CO_2CH_2		*meta*	87
18e	CO_2CH_2		*para*	17
17	CH_2OCH_2	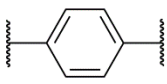		7.2

[a] Inhibitory activity against human DPP-4 was measured using Gly-Pro-*p*NA as a substrate.

To understand the binding modes of these series of quinoline- and pyridine-based carboxylic acids, the corresponding carboxamides were evaluated for DPP-4 inhibitory activity (Table 3). As a result, all the representative carboxamides **28a–c** exhibited potent inhibitory activity, which indicates that polar substituents

are favorable as the C-terminal moiety. Interestingly, these compounds tend to show slightly less potent inhibitory activity than that of the corresponding carboxylic acids (ca. 3 to 5-fold). The results suggest that the salt bridge formation would be involved in the stronger interaction between the enzyme and the inhibitors targeting the S1' pocket.

Table 3. DPP-4 Inhibitory Activity of Carboxamides **28**

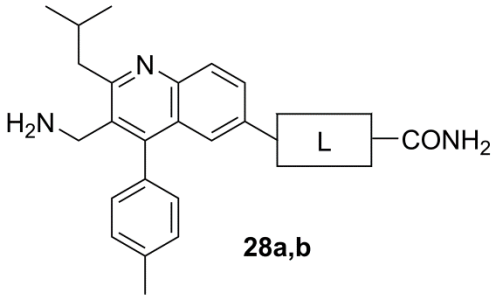

28a,b

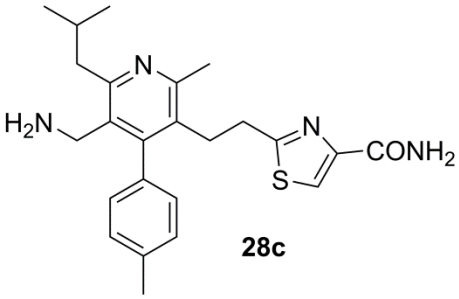

28c

Compound	L	Additive	DPP-4 IC_{50} (nM)[a]
28a	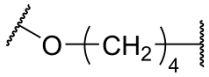	none	13
28b	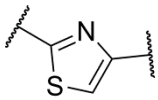	2HCl	2.1[b]
28c		2HCl	8.5

[a] Inhibitory activity against human DPP-4 was measured using Gly-Pro-*p*NA as a substrate. [b] IC_{50} value of the corresponding methyl ketone (**28d**) was 8.7 nM.

Next, compounds were docked into the DPP-4 model. Figure 4 displays the model of **4** as a representative. Their core rings showed an excellent overlay with that of isoquinolone **1**, predicting a very limited potency loss in each interaction between the 2-, 3-, and 4-substituents and their target residues. The thiazole ring of **4** would be positioned appropriately for a π–π stacking interaction with the benzene ring of Tyr547 (ca. 4 Å distance in **4**).[21] The stacking ring linkers would consequently make the carbonyl oxygen oriented to the amino nitrogen of Lys554 in a suitable distance for a salt bridge interaction (2.8 Å). Interestingly, the docking model suggested that **4** would make no direct interaction with the catalytic serine (Ser630). Taken together with the SAR results, it is strongly suggested that **4** would exhibit the highly potent subnanomolar inhibition

by employing the hydrophobic interaction with Tyr547 as well as the salt bridge interaction with Lys554 without the interaction with the catalytic residue.

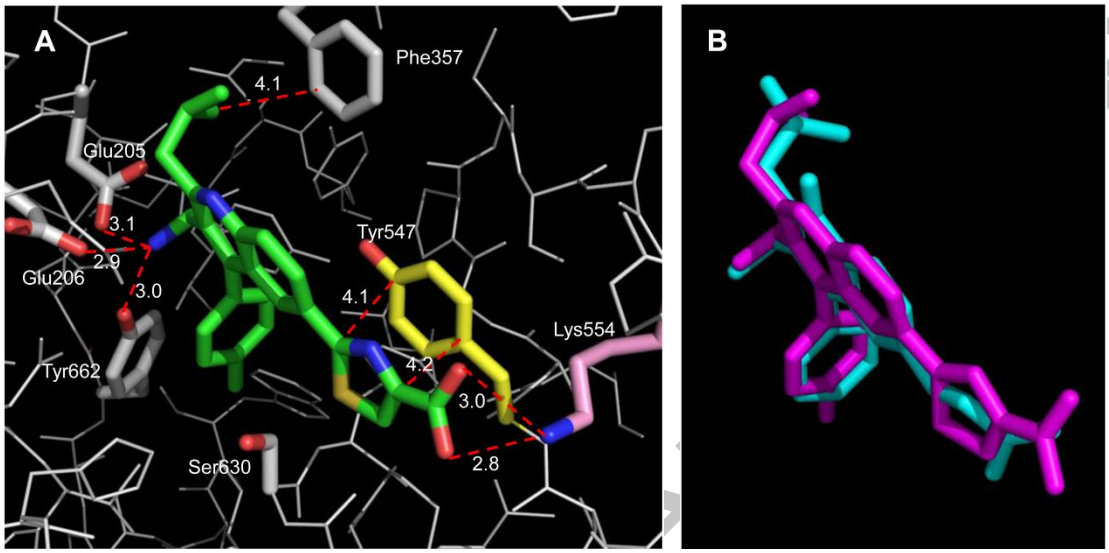

Figure 4. Docking study of compound **4** with DPP-4 protein. (A) Lys554 (pink), Tyr547 (yellow), and other amino acids (gray) in the binding site of **4** (green carbons). Major interactions are depicted as red dotted lines. Distances in angstroms. (B) Superimposition of **4** (magenta) onto X-ray cocrystal structure of **1** (cyan).

In addition to the promising DPP-4 inhibition profiles, reduced DPP-8 inhibition was consistently found in analogues targeting Lys554. It is assumed that the isozyme selectivity is induced by the sequence differences between the two enzymes in S2 pocket (Phe630 in DPP-4 vs His in DPP-8) and in S1' pocket (Lys554 in DPP-4 vs Leu in DPP-8). Our templates utilize Phe357 to make an indispensable hydrophobic interaction with the isobutyl group and generally lead to high selectivity against the isozyme. It is consistent that pyridine-based inhibitor **3**[15] shows very low DPP-8 inhibitory activity with an IC_{50} value of 11 μM (500-fold selective for DPP-4) most likely by the unfavorable hydrophobicity of the 2-isobutyl group.[22] By adding a polar substituent that reaches Lys554 onto the 6-carboxy group of **3**, compound **18e** showed further potency reduction for DPP-8 (IC_{50} > 100 μM). A similar result has been reported in quinoline **2**, which can make a hydrogen bonding to Lys554.[14] The potency losses in the analogues targeting Lys554 could be explained by the other sequence difference in S1' pocket, and the introduced hydrophilic substituent (e.g. carboxy and carbonyl groups) would be unfavorable under the hydrophobic environment in the S1' pocket of DPP-8. Thus, the proposed pharmacophore would also provide an attractive feature of higher selectivity against DPP-8.

Representative pharmacological profiles are shown in Figures 5 and 6. An oral dose of 1 mg/kg of **4** induced >50% inhibition of plasma DPP-4 activity during 6 h in an ex vivo test in Sprague Dawley rats

(Figure 5). In an oral glucose tolerance test in female Wistar fatty rats, **4** significantly reduced glucose excursion and enhanced insulin secretion after oral glucose load at 1 mg/kg (Figure 6). These ex vivo and in vivo results clearly demonstrate the potential for our design strategy to yield a new lead with in vivo efficacy.

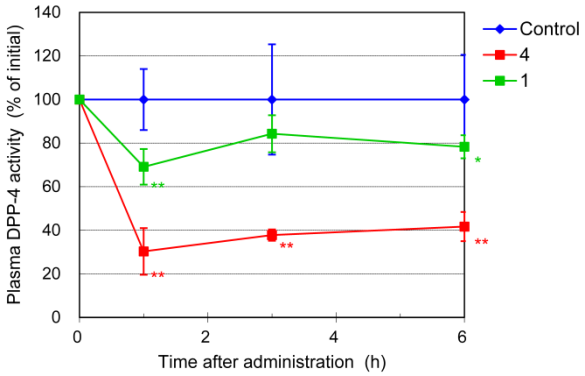

Figure 5. Ex vivo study of compound **4** in Sprague-Dawley rats. Data points and error bars indicate means and SD, respectively, of the residual DPP-4 activity in rat plasma after administration of 1 mg/kg of compound (n = 5). * $p < 0.05$, ** $p < 0.001$ versus control by Dunnett test. Compound **1** was used as a positive control for the experiment.

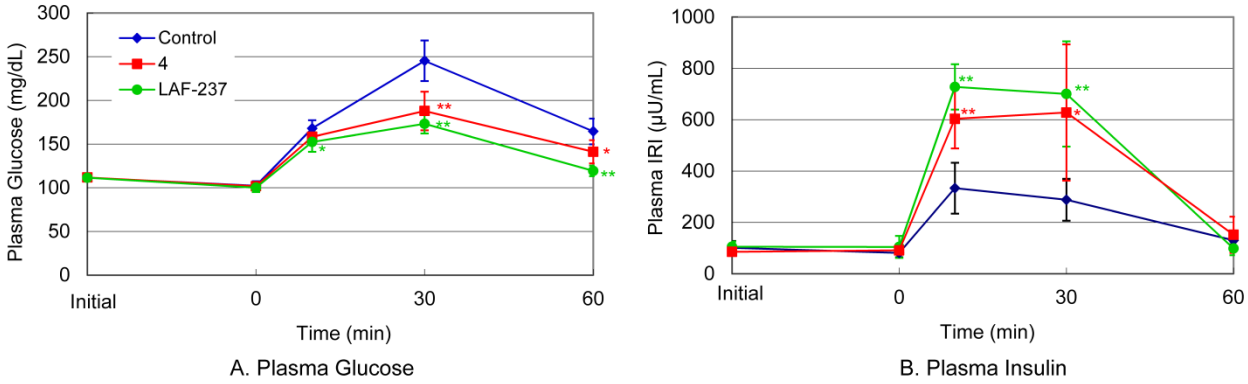

Figure 6. Oral glucose tolerance test of compound **4** in female Wistar fatty rats. Plasma glucose (A) and plasma insulin levels (B) of rats administered 1 mg/kg of compound or 0.5% MC 60 min before oral glucose load (1 g/kg). Data points indicate means, and the error bars indicate SD (n = 6). * $p < 0.05$, ** $p < 0.01$ versus control by Dunnett test. LAF-237 was used as a positive control for the experiment.

In summary, we have designed a series of carboxylic acids incorporated in quinoline-based and pyridine-based templates of DPP-4 inhibitors. In the design, the terminal carboxy groups are appropriately directed toward Lys554 in the S1' pocket to form a salt bridge, suggesting the importance of the hydrophobic interaction between the aromatic ring linkers and Tyr547. The representative quinoline (**4**) and pyridines (**16a**, **16b**, and **17**) demonstrated subnanomolar to nanomolar inhibition. Interestingly, the docking studies suggested that these potent DPP-4 inhibitors have no direct interaction with the active site residue Ser630 in contrast to

many of the reported inhibitors. Furthermore, the interaction with Lys554 can contribute to the isozyme selectivity against DPP-8. Taken together, the design strategy using our templates would be useful to explore a novel design for DPP-4 inhibitors having a distinct structure with a unique binding mode

Acknowledgements

The authors would like to thank Nobuo Cho for critical reading of the manuscript and for useful suggestions to improve it. The authors would also like to thank Harumi Hattori and Yusuke Kamada for a statistical analysis of biological data and Koji Takeuchi, Yu Momose, Yuji Ishihara, Shigenori Ohkawa, Takashi Sohda, and Akio Miyake for helpful discussions throughout the study.

A. Supplementary data

Supplementary data associate with this article can be found, in the online version, at http://....

References and Notes

1. WHO. Global Report on Diabetes. World Health Organization Library Cataloguing; 2016.
2. NCD Risk Factor Collaboration. *Lancet.* 2016;387:1513.
3. Edwards CM. *Ann Med.* 2005;37:314.
4. Salvatore T, Carbonara O, Cozzolino D, Torella R, Sasso FC. *Curr Diabetes Rev.* 2007;3:15.
5. Mentlein R, Gallwitz B, Schmidt WE. *Eur J Biochem.* 1993;214:829.
6. Drucker DJ. *Expert Opin Investig Drugs.* 2003;12:87.
7. Crepaldi G, Carruba M, Comaschi M, Del Prato S, Frajese G, Paolisso G. *J Endocrinol Invest.* 2007;30:610.

8. Scheen AJ. *Expert Opin Pharmacother.* 2015;16:43.
9. Kaku K. *Expert Opin Pharmacother.* 2015;16:2539.
10. Nabeno M, Akahoshi F, Kishida H, et al. *Biochem Biophys Res Commun.* 2013;434:191.
11. Watanabe YS, Yasuda Y, Kojima Y, et al. *J Enzyme Inhib Med Chem.* 2015;30:981.
12. Arulmozhiraja S, Matsuo N, Ishitsubo E, Okazaki S, Shimano H, Tokiwa H. *PLoS One.* 2016;11:e0166275.
13. Banno Y, Miyamoto Y, Sasaki M, et al. *Bioorg Med Chem.* 2011;19:4953.
14. Maezaki H, Banno Y, Miyamoto Y, et al. *Bioorg Med Chem.* 2011;19:4482.
15. Miyamoto Y, Banno Y, Yamashita T, et al. *J Med Chem.* 2011;54:831.
16. See supplementary SAR information Table S1.
17. Ikuma Y, Hochigai H, Kimura H, et al. *Bioorg Med Chem.* 2012;20:5864.
18. Ikuma Y, Hochigai H, Kimura H, et al. *Bioorg Med Chem.* 2015;23:779.
19. Miyamoto Y, Banno Y, Yamashita T, et al. *Bioorg Med Chem.* 2011;19:172.
20. Tsuzuki S, Honda K, Uchimaru T, Mikami M, Tanabe K. *J Am Chem Soc.* 2002;124:104.
21. Rummey C, Metz G. *Proteins.* 2007;66:160.

Graphical Abstract

Design of potent dipeptidyl peptidase IV (DPP-4) inhibitors by employing a strategy to form a salt bridge with Lys554

Leave this area blank for abstract info.

Hironobu Maezaki*, Michiko Tawada, Tohru Yamashita, Yoshihiro Banno, Yasufumi Miyamoto, Yoshio Yamamoto, Koji Ikedo, Takuo Kosaka, Shigetoshi Tsubotani, Akiyoshi Tani, Tomoko Asakawa, Nobuhiro Suzuki, and Satoru Oi

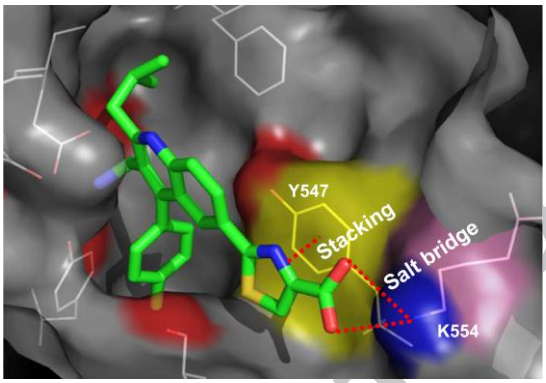

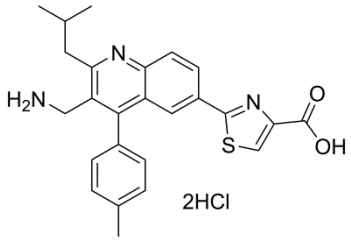

4 IC_{50}: 0.38 nM